Full Paper

Urea Sensitive Impedimetric Determination Based on Fluorinated-Tin Oxide Electrode Modified with Novel Cadmium Sulfide Nanorod Transducer: A Unique Mechanism

Mohaddeseh Mikani,[1] and Reza Rahmanian [2,*]

[1]*Department of Food Science & Technology, Iranian Research Organization for Science and Technology (IROST), Tehran, Iran*
[2]*Young Researchers and Elite Club, North Tehran Branch, Islamic Azad University, Tehran, Iran*

*Corresponding Author, Tel.: +982188409098

E-Mail: Uniquerezarahmaneian@gmail.com

Abstract- As an innovative approach, cadmium sulfide (CdS) nanorod was synthesized and applied to modify a fluorinated-tin oxide conducting glass (SnO_2:F) as a matrix for urea bioelectrode. Besides, urease (Urs) was exploited as a particular enzyme for urea recognition with excellent accuracy and precision via a unique mechanism. In this case, Urs has immobilized physically over the matrix superficial (CdS/SnO_2:F) electrode. Initially, the fabricated CdS nanorods qualities were deliberated by scanning electron microscopy (SEM), energy-dispersive X-ray spectroscopy (EDX), and X-ray diffraction (XRD) analyses while the fabricated Urs/CdS/SnO_2:F bioelectrode was considered employing electrochemical impedance spectroscopy (EIS) and cyclic voltammetric (CV) techniques. The modified bioelectrode efficiency for urea analysis was presented while the parameters affecting the peak current were improved. Under the best circumstances, the novel bioelectrode illustrated a linear response over an extensive range of urea concentrations (5 to 200 mg dL^{-1}), the detection limit was 3 mg dL^{-1}. The projected Urs/CdS/SnO_2:F bioelectrode has a fast response time of less than 3 s. The technique was exploited to the urea measurement in pharmaceutical preparation and human serum samples, and suitable outcomes were acquired.

Keywords- Urea; Cadmium sulfide nanorod; Disposable bioelectrode; Electrochemical performance; Human serum

1. INTRODUCTION

Electrochemical approaches have been established to be very subtle for the organic molecules measurement [1-5]. These approaches are easier, faster and cheaper than traditional techniques. Furthermore, the modified electrode has respectable sensitivity, electro catalytic activity, and selectivity; it has correspondingly a low detection limit compared to unmodified electrodes [5-9]. Presently, it is essential to refining unique sensing resources such as nanostructures [10-13] talented to improve the analytical features of the modified electrode transducer [13-15]. Nanomaterials display many profits such as a great surface area to volume ratio and high activity and have become one of the most talented constituents [16-22]. Nanosized particle-modified electrodes have developed as a talented alternative for the mineral and organic materials quantification [3,7,9]. The nanorods have some distinct profits such as high mass transport rate, low detection limits, low solution resistance influence, and better signal-to-noise proportion compared to the norm macroelectrodes [4,9]. Cadmium Sulfide (CdS) is one of the most widely deliberated semiconducting materials belonging to the II-VI group [23-25]. It has exceptional chemical assets owing to the size consequence. In this scheme, CdS nanorods were exploited for the urea sensor transducer surface which aids the electron transmission, enriches the operative electroactive surface zone and improves the detection limit of urea.

Currently, disposable bioelectrode have applied by electroanalysts due to their capacity to afford large-scale construction of electrodes possessing features such as portability, high versatility, and cost-effectiveness [26-28]. Disposable sensors including modified bioelectrode have led to advanced potentials for the analyte measurement. At the traditional electrode, the solid electrodes are very frequently suffered from the fouling effect due to the oxidized products accumulation on the electrode platform, which consequences in rather reduced selectivity and sensitivity. Excellent electrochemical properties of F-doped SnO_2 conducting glass modified with cadmium sulfide (CdS) nanorod ($CdS/SnO_2{:}F$) after urease (Urs) immobilization ($Urs/CdS/SnO_2{:}F$) proposes the sensitive electrochemical measurement of urea with respectable stability, low detection limit, and rapid response. Urea (carbonyl diamide [$(NH_2)_2CO$]) is a vital molecule that exists in nature and its determination is of utmost significance not only for medical goals but likewise from environmental viewpoints. In the human body, urea exists in exact amounts (normal range is 15–40 mg dL^{-1}) in several pathological fluids such as urine, serum, and blood [29-36]. In this case, under optimized conditions, electrochemical performances exhibits a linear response for urea over a concentration range of 5 to 200 mg dL^{-1} with a correlation coefficient (R^2) of >0.99, detection limit (LOD) (S/N = 3) 3 mg dL^{-1}. The suggested $Urs/CdS/SnO_2{:}F$ bioelectrode offered a quick response time of less than 3 s and retained exceptional stability for more than 16-weeks. A quick response of a constructed sensor can typically permit real-time investigation of real samples.

2. EXPERIMENTAL

2.1. Materials

All used chemicals were of analytical reagent grade and acquired from Merck (Darmstadt, Germany) or Aldrich (Chemical Co., Milwaukee, WI, USA). Double-distilled water was employed throughout the experimentations. Phosphate buffer solution (PBS) was ready from K_2HPO_4 and KH_2PO_4 and the pH was attuned to 5.5. Urs solution was organized in PBS, 0.1M pH 5.5 comprising 100 units for 3h. A stock urea solution urea was organized in 0.1M PBS and retained at 4 °C. The standard low urea concentrations were prepared earlier the measurement. SnO_2:F transparent conducting glasses with a size of 25×35 mm, the thickness of 2.2 mm, and the 10 Ω per square sheet resistance were exploited which were acquired from Wuhan Lattice Solar Energy Technology Co. Ltd. Conducting glass substrates were cleaned under ultrasonic treatment (5 min in alcohol, 5 min in acetone), washed plentifully with water, and finally preserved for 2 min in a 45% nitric acid solution formerly drying in a nitrogen atmosphere.

2.2. Apparatus

The electrochemical experiments were achieved using an Autolab potentiostat/galvanostat (PGSTAT 302N, Eco Chemie, the Netherlands) while working modified electrode as Urs/CdS/SnO_2:F, an SCE electrode as a reference electrode and a Pt wire as a counter electrode. General-purpose electrochemical system software was used to control the system. The electrochemical cell was positioned in a Faraday cage to reject every environmental stray effect. For EIS quantification, 10 mV peak- to-peak AC amplitude was exploited, a 100 kHz to 1000 mHz frequencies range was scanned, and the impedances were documented. The analysis of EIS data was achieved using Zview/Zplot (Scribner Associates, Inc.) based on Macdonald's algorithm (LEVM 7) exploiting a complex non-linear least square (CNLS) approximation method [37]. The morphology of the products was observed using a Philips XL30 scanning electron microscope (SEM). Before SEM analysis, samples were overloaded on a gold film equipped by an SCD005 BAL-TEC Sputter Coater. Dip coater (Model: KP-4001) was employed for thin film construction. The pH values were measured by a Metrohm 710 pH meter. X-ray diffraction (XRD) studied were directed on a Rigaku D/max 2500 V instrument with a graphite monochromator and a Cu target.

2.3. Matrix construction

By a simple wet chemical technique, the CdS nanorods were produced under reflux circumstance. Cadmium acetate, thioacetamide (TAA), and thioglycolic acid (complexing agent) were applied as raw materials. In a typical production, cadmium acetate (1.066 g) was dissolved into distilled water (100 mL) in the round-bottomed flask (250 mL), followed by addition of thioglycolic acid (5 mL) [23] and was refluxed for 1 h at 100 °C. Next, 0.6010 g

TAA (50 mL) was rapidly injected to the overhead solution and the whole solution was refluxed for 6 h at 100 °C. Besides, it was cooled to ambient temperature. The precipitate was cleaned with absolute ethanol numerous times to eliminate any ionic residual and then dried in the oven for 6 h at 60 °C.

Nanorods are an exceptional component to be deliberated and perfect candidates for many requests due to their shape anisotropy (physical properties). It was revealed that the nanorod's capability was improved as compared to sphere-shaped particles. This is due to the aspect ratio progress of the particle cause the improved of surface plasmons excitation in the nanoparticles. Mainly, the strength of the dipole moment is within a nanoparticle due to the surface plasmons incrementing. Consequently, a growth of surface plasmons leads to the improvement of the electrical field in nanorods as compared to sphere-shaped particles. Fabricated CdS nanorods were dip-coated and applied to modify a SnO_2:F as a matrix for urea bioelectrode.

3. RESULTS AND DISCUSSION

3.1. Characterization study

The CdS SEM images (Fig. 1A, B) with different magnification accompany with energy dispersive X-ray spectroscopy (EDX) analysis (Fig. 1C) show CdS nanorod construction. Highly uniform nanorod thin film on the SnO_2:F electrode surface gives great surface areas with the nanorods about sizes<100 nm (Fig. 1D). The surface analysis of the CdS nanorod SEM image offered a distribution design and a pores intensity which is supposed to show a vital character in enzyme immobilization. From numerous approaches projected for the enzyme immobilization, the greatest usual is on the solid carriers adsorption. The most significant benefit of this immobilization is that a carrier's extensive gamut can be exploited and that the enzymes of practically every class can be immobilized. Similarly vital is the fact, that this immobilization leaves the enzyme construction intact, which permits enzymes to preserve their activity and correspondingly facilitates the substrates transport to the enzyme's active midpoint.

For the crystal structure CdS nanorods exploration, XRD analysis was deliberated. Advantages of XRD analysis are listed as (i) Materials fast identification, (ii) Easy sample preparation, (iii) Large library of known crystalline structures. In this study, the angle 2θ ranged from 10° to 80°, with a step of 0.02°. The scan step time was 0.5 s and the measurement temperature was 25°C. In this case, XRD studies were performed on the optimal products CdS nanorods to estimate the chemical composition and the consequences (Fig. 1E) exposed robust main peaks in a moderately smooth baseline [23-25]. As for CdS nanorods, all of the diffraction peaks can be assigned to CdS nanorods structure (JCPDS No. 41-1049), no more diffraction peaks are perceived, representing the CdS formation, which was correspondingly detected in preceding documents [23,25].

In this circumstance, Urs adsorption was performed by soaking the CdS/SnO$_2$:F in a PBS, 0.1M, pH 5.5 containing 0.2 mg mL^{-1} Urs at ambient temperature for 3 h. The CdS/SnO$_2$:F was kept in PBS until procedure. The Urs attachment with CdS/SnO$_2$:F was projected to be forced by the difference in their isoelectric points (IEP), which delivers Urs/CdS/SnO$_2$:F bioelectrode [2,7,9,10,29]. Step by step checking of Urs/CdS/SnO$_2$:F bioelectrode construction was achieved employing electrochemical methods such as current vs. electrochemical impedance spectroscopy (EIS) and cyclic voltammetric (CV) procedures. After finishing these steps, the fabricated bioelectrode was employed as the working electrode for urea measurement exploiting electrochemical assessment.
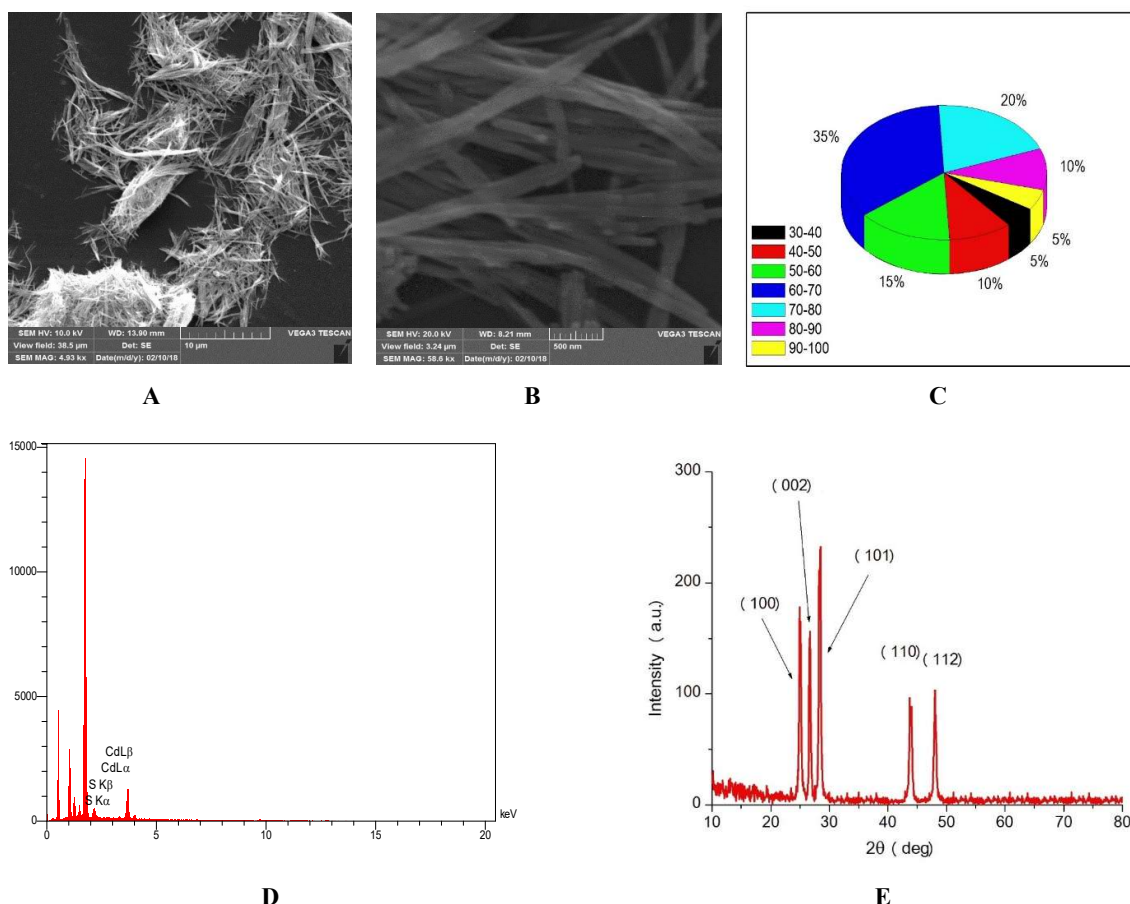

Fig. 1. The SEM images of the (A, B) CdS nanorod with various magnifications accompany with (C) particle size distribution pie chart of CdS nanorod, (D) CdS nanorod EDX analysis, and (E) The XRD spectrum for CdS nanorod

3.2. Dip-coating parameters optimization

Dip-coating is no doubt the quick procedure to prepare thin films with the maximum control degree, making it extremely appropriate for bioelectrode platform fabrication. Dip-coating method was employed to create CdS/SnO$_2$:F electrode. Consequently, the SnO$_2$:F electrode

with tap pasted on the whole back and the upper front was fixed on the dip coater, immersed into the 10 mL ethanolic dispersion lifted with speeds of 3-300 mm min^{-1}and with speed of 600 mm s^{-1}, correspondingly. For gaining optimum CdS/SnO$_2$:F CV response at E=0.2 V for urea 200 mg dL^{-1}, nanorods were applied, and several parameters of dip-coating, comprising lifting speed (3-300 mm min^{-1}), CdS nanorods concentration (1-5 g L^{-1}), and dipping number (1, 2, 3, 4 and 5) were explored.

To investigate the lifting speed effects, 3-300 mm min^{-1} lifting speeds were employed by fixing the nanorods concentration to be 4 g L^{-1}, and the dipping number to be 4 (Fig. 2A). To investigate the effects of nanorods concentration on the CdS/SnO$_2$:F electrode performance, nanorods concentration 1-5 g L^{-1} were exploited by fixing 200 mm min^{-1} lifting speed, and the 4 dipping number (Fig. 2B). To study the dipping number influence on the device performance, 1, 2, 3, 4 and 5 dipping numbers were employed by fixing the lifting speed to be 200 mm min^{-1}, and the nanorod concentration to be 4 g L^{-1} (Fig. 2C).

For obtaining CdS/SnO$_2$:F thin film optimum conditions, as an exceptional bioelectrode platform for the maximum electrochemical response, were deliberated in continue as 200 mm min^{-1}, 4 g L^{-1}, 4 for lifting speed, nanorods concentration, and dipping numbers, respectively. The designated quantities were preferred as best values to attain CdS/SnO$_2$:F thin film with the uniform nanorod morphology with appropriate sites for enzyme immobilization accompany with proper conductivity while attaining a best bioelectrode electrochemical response.
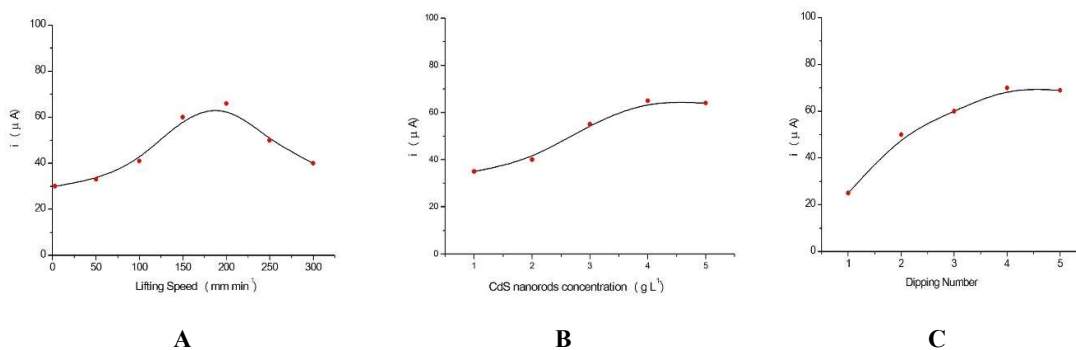

| **A** | **B** | **C** |

Fig. 2. Effect of (A) Lifting speeds, (B) Nanorods concentration, and (C) Dipping number on the Urs/CdS/SnO$_2$:F bioelectrode final CV current response at E=0.2V for urea 200 mg dL^{-1}

3.3. Impedimetric and voltammetric profiles of Urs/CdS/SnO$_2$:F bioelectrode

EIS values can exhibit the interfacial info through the modification procedure. The semicircle diameter of the Nyquist plot illustrates the electron transfer resistance (R$_{et}$), which is resulted from the electron transfer of the redox probe [Fe(CN)$_6$]$^{3-/4-}$. The AC voltage amplitude was fixed as 5 mV. By exploiting 1 mol L^{-1} KNO$_3$ and a 5.0 mmol L^{-1} [Fe(CN)$_6$]$^{3-/4-}$ solution as the electrochemical probe with 100,000 to 0.1 Hz frequencies range, the Nyquist plots of several modified electrodes were documented with the consequences showed in Fig.

3A. At this point, Z′ and Z″ are the real variables and the negative value of the impedance imaginary variable. Because of SnO_2:F bare electrode has the maximum conductivity due to inherent electrode possessions (not modified), the R_{et} value of SnO_2:F bare electrode was 1.15 kΩ value. Maximum R_{et} value (92 kΩ) was acquired on final modified structure (Urs/CdS/SnO_2:F). The progressively augmented the interfacial resistance during modification ascribed to insulating characteristics of Urs respect to SnO_2:F. Furthermore, the CV investigation of the layer by layer assembly of Urs/CdS/SnO_2:F in urea-free PBS containing 5.0 mmol L^{-1} $[Fe(CN)_6]^{3-/4}$ and 1 mol L^{-1} KNO_3 is revealed in Fig. 3B. The anodic peak current magnitude for CdS/SnO_2:F electrode (1013 μA) is lower than that of bare SnO_2:F electrode (1518 μA) exposes that CdS nanorod proves a little obstruction to the electron transfer from/to the electrode surface due to its semiconducting features. The peak current response magnitude for Urs/CdS/SnO_2:F bioelectrode displays decreases in electron transfer from/to the electrode surface (33.21 μA) which is shown the Urs insulating characteristics [10,29]. These consequences are consistent with the stepwise layer by layer assembly studying outcomes that were obtained by EIS tests.
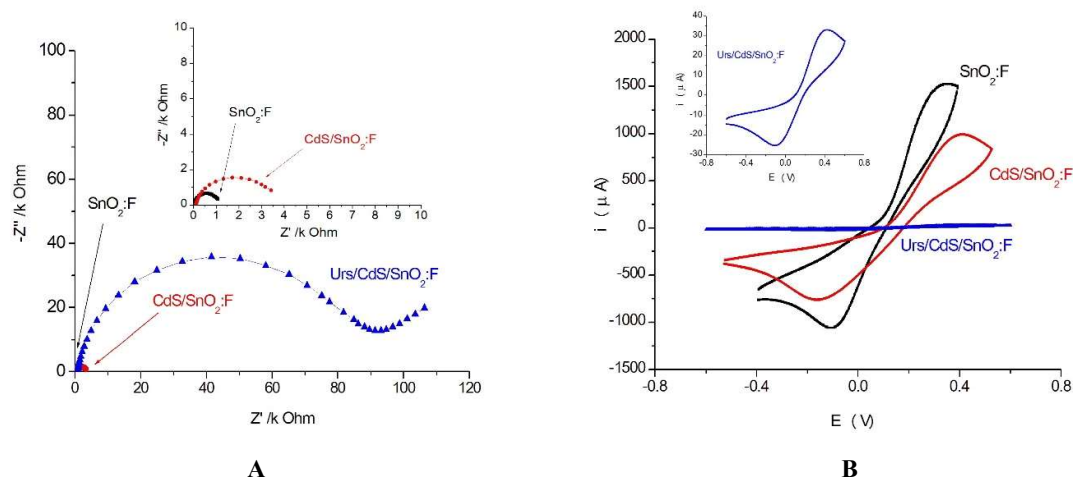

Fig. 3. (A) The Nyquist plots (-Z″ *vs.* Z′), and (B) Cyclic voltammograms at the scan rate of 0.1 V s^{-1} obtained in urea-free PBS (pH 5.5) containing 5.0 mM $[Fe(CN)_6]^{3-/4-}$ as redox probe and 1 mol L^{-1} KNO_3 for SnO_2:F, CdS/SnO_2:F, Urs/CdS/SnO_2:F. The inset in (A) shows the magnified Nyquist plots of CdS/SnO_2:F and SnO_2:F electrodes. The inset in (B) shows the magnified voltammogram of Urs/CdS/SnO_2:F bioelectrode

Fig. 4A illustrates the cyclic voltammograms, in PBS (pH 5.5) containing 5.0 mM $[Fe(CN)_6]^{3-/4-}$ as redox probe and 1 mol L^{-1} KNO_3, obtained for Urs/CdS/SnO_2:F bioelectrode as a urea concentration function. It can be distinguished that the peak oxidation current progressively improves with an growth in urea concentration from 0 to 200 mg dL^{-1} for the bioelectrode. The progress in the oxidation current is due to an improved biochemical reaction happen on the bioelectrode surface with increasing urea concentration. The urea bioelectrode

response without immobilization of enzyme (Urs) was furthermore examined by carrying out a control experiment in which sensing response for urea was deliberated without Urs immobilization on the surface of CdS/SnO_2:F electrode. It was established that no change in the redox peak currents was detected in the cyclic voltammograms for the CdS/SnO_2:F electrode upon various urea concentrations addition from 5 to 200 mg dL^{-1} to the PBS (pH 5.5) containing 5.0 mM $[Fe(CN)_6]^{3-/4-}$ as redox probe and 1 mol L^{-1} KNO_3 solution (Fig. 4B). Accordingly, in Fig. 4C, the growth in CV oxidation current perceived in the biosensing reaction concerning Urs/CdS/SnO_2:F bioelectrodes with varying urea concentrations is particularly due to the bioelectrocatalytic oxidation of urea in the immobilized Urs presence and not due to the direct oxidation of urea on the surface of CdS/SnO_2:F electrode. The perceived consequences confirm that enzyme (Urs) shows a significant role as an electrocatalyst in the existing exploration and the matrix of CdS/SnO_2:F delivers an efficient media for conformal immobilization of Urs.

The calibration curve (Fig. 4C) obtained for Urs/CdS/SnO_2:F bioelectrode have been fitted to the linear regression equations and is given as follows: Current (μA)= 0.17 (± 0.01) × urea concentration (mg dL^{-1}) + 35.92 (± 0.72); R^2=0.9914. The linear enhancement in the peak oxidation current with an growth in urea concentration proposes that CdS/SnO_2:F platform provides a favorable media to the immobilized Urs enzyme. The sensitivity for Urs/CdS/SnO_2:F bioelectrodes are very appropriate. In addition, the detection limit of 3 mg dL^{-1} was reported.

The conceivable biochemical reactions schematic occurring at the surface of the organized bioelectrode is revealed in Fig. 5. In PBS solution comprising 5 mM $[Fe(CN)_6]^{3-/4-}$ as the redox mediator species, analyte of various concentrations is added which upon oxidation in the immobilized Urs presence gives rise to chemical products like ammonia (NH_3) and carbon dioxide (CO_2), and consequently through this process the Urs gets reduced. The Urs activity is owed to the SH groups attendance on its active position that can be oxidized as well as reduced by the biochemical feedback. Hereafter, the reduced Urs loses electrons and gets oxidized. The Fe^{3+} ions present in the PBS solution as a result of $[Fe(CN)_6]^{3-/4-}$ redox mediator species capture the released electrons in the vicinity of the bioelectrode surface and reduces to Fe^{2+} ions. Additional, when Fe^{2+} ions oxidize back to Fe^{3+} ions the released electrons are transferred to the underneath SnO_2:F layer of the bioelectrode via an efficient CdS nanorod matrix possessing fast electron communication feature and thus completing the conduction path.

The above-discussed electron transfer procedure takes place through the forward scan of the voltammograms and during the reverse scan, the whole procedure gets repeated in the opposite manner as exposed in Fig. 4A. Therefore, the urea catalytic oxidation by the Urs comprises attain or loss of electrons consequently completing a redox reaction and the identified growth in the oxidation peak current with improving urea concentration is recognized to the growth in the number of the released electron during oxidation.
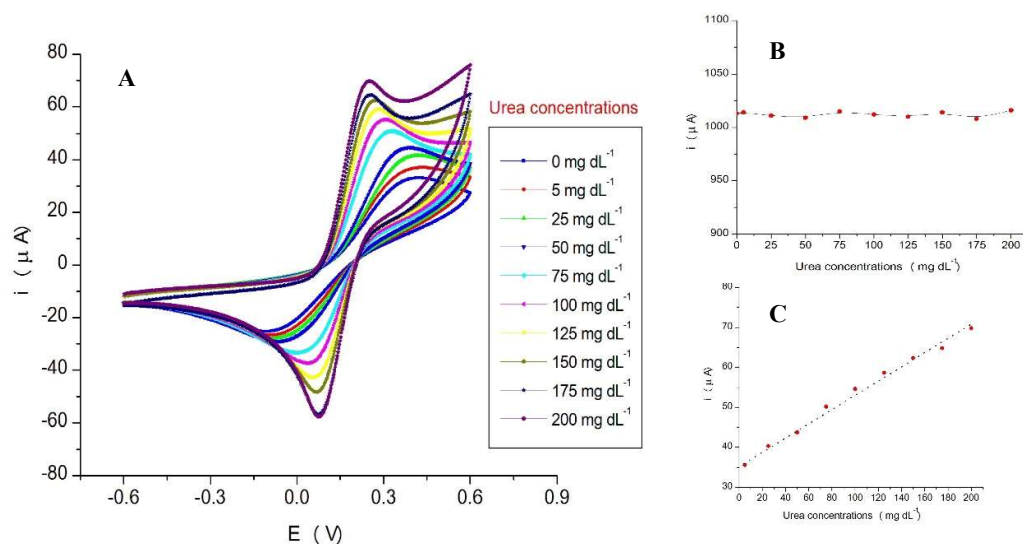
Fig. 4. (A) Cyclic voltammograms at the scan rate of 0.1 V s^{-1} in PBS (pH 5.5) containing 5.0 mM [Fe(CN)$_6$]$^{3-/4-}$ as redox probe and 1 mol L^{-1} KNO$_3$ obtained on the Urs/CdS/SnO$_2$:F bioelectrode in the presence of different concentration of urea: 5 to 200 mg dL^{-1}. (B) Oxidation peak current observed on the CdS/SnO$_2$:F electrodes in PBS (pH 5.5) containing 5.0 mM [Fe(CN)$_6$]$^{3-/4-}$ as redox probe and 1 mol L^{-1} KNO$_3$ with varying urea concentrations, and (C) Variation of oxidation peak current in PBS (pH 5.5) containing 5.0 mM [Fe(CN)$_6$]$^{3-/4-}$ as redox probe and 1 mol L^{-1} KNO$_3$ as a function of urea concentration, which represents calibration curve
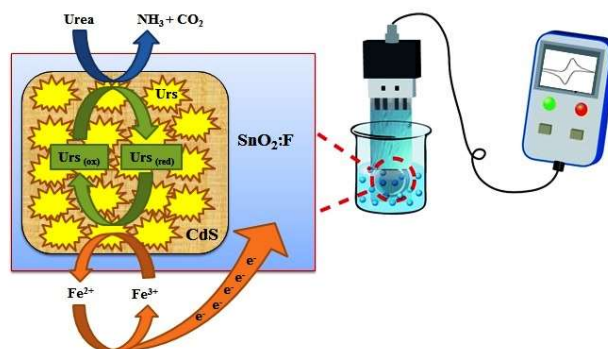

Fig. 5. Schematic of the electron transfer process occurring at the surface of the Urs/CdS/SnO$_2$:F bioelectrode in the presence of urea in PBS (pH 5.5) containing 5.0 mM [Fe(CN)$_6$]$^{3-/4-}$ as redox probe and 1 mol L^{-1} KNO$_3$

The Urs/CdS/SnO$_2$:F bioelectrode electrochemical response has been impedimetricly determined as a urea concentration function. As revealed in Fig. 6A, the R$_{ct}$ magnitude reduces on the urea addition from 5 to 200 mg dL^{-1} to the PBS (pH 5.5) containing 5.0 mM [Fe(CN)$_6$]$^{3-/4-}$ and 1 mol L^{-1} KNO$_3$. The fast response displays that the CdS nanorod structure

matrix produces a very low mass transport barrier and outcomes in a quick diffusion from solution to the enzyme with the protection of its bioactivity.

The impedimetric training obviously designates that the process stated in CV investigation section is a reversible procedure and supports the Urs–urea enzymatic catalysis. From impedimetric trainings and step by step studies, it is confirmed that the fabricated bioelectrode can be re-used. The calibration curve was achieved for urea at the Urs/CdS/SnO$_2$:F bioelectrode by checking its R_{ct} responses ($|\Delta R_{ct}|=|R_{ct\ urea}-R_{ct\ blank}|$). Fig. 6B displays a working curve shown in a linear scale $\Delta R_{ct}(k\Omega)= 0.29\ (\pm0.01) \times$ urea concentration (mg dL^{-1}) + 33.42 (±0.82); $R^2=0.9916$ in a concentration range of 5 to 200 mg dL^{-1} of urea. The Urs/CdS/SnO$_2$:F bioelectrode displays a detection limit of 3 mg dL^{-1} for urea and sensitivity of 0.29 kΩ per mg dL^{-1} with a linear range within 5 to 200 mg dL^{-1}. These consequences confirm that CdS nanorod thin film matrix affords a smart media for enzyme immobilization to preserve its anticipated natural activities. In conclusion, for the urea concentrations case where the voltammetric waves merge and migrate out of the potential window, EIS is exposed to be a more appropriate technique, due to the perceived linear increases in R_{ct} with growing concentration.
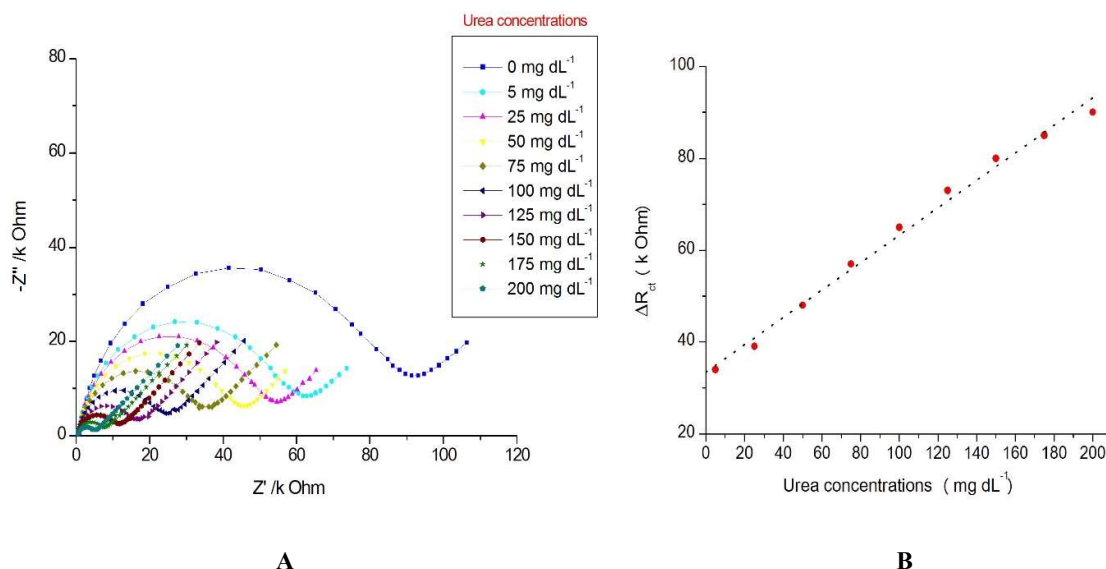

Fig. 6. (A) The Nyquist plots (-Z″ *vs.* Z′), obtained on the Urs/CdS/SnO$_2$:F bioelectrode in PBS (pH 5.5) containing 5.0 mM [Fe(CN)$_6$]$^{3-/4-}$ as redox probe and 1 mol L^{-1} KNO$_3$ in the presence of different concentration of urea, (B) Variation of charge transfer resistance (ΔR ct) as a function of urea concentration represents calibration curve

3.4. Effect of pH

At a specific pH, once colloidal particles in a solution carry no net charge, the inter-particle repulsive forces are inattentive leading to the colloidal solution to be least steady. This dispersion medium pH is recognized as IEP [38]. This IEP is one of the rudimentary particles

characteristics that carry a charge (for example biomolecules). This aids in defining a sign of the net charge for various pH values. The notable effort to immobilize Urs onto the electrode was through spontaneous adsorption, which occurs by electrostatic adsorption of positively charged Urs (IEP ~ 5.9) and negatively charged CdS (IEP ~ 3.7-4.6) [7,9,10,29] at pH 5.5. The finest buffer pH for urea hydrolysis by Urs was deliberated as 5.5, at which Urs enzyme preserves its natural structure and activity that is essential to progress detection limit and sensitivity for urea detection (Fig. 7A).

3.5. Effect of salt concentration

The supporting electrolytes effect with various concentrations such as KNO_3, KI, $NaNO_3$, and $KClO_4$ on the CV peak current of 200 mg dL^{-1} urea in PBS (pH 5.5) containing 5.0 mM $[Fe(CN)_6]^{3-/4-}$ as redox probe and 1 mol L^{-1} KNO_3 was correspondingly checked by the test solution. The supporting electrolyte concentration altered between 0.0 and 1.0 mol L^{-1} in the test solution. The consequences offered that the technique sensitivity and CV peak current improved by rising KNO_3 salt concentration as a supporting electrolyte (Fig. 7B). The 1.0 mol L^{-1} KNO_3 designated as the optimum concentration.
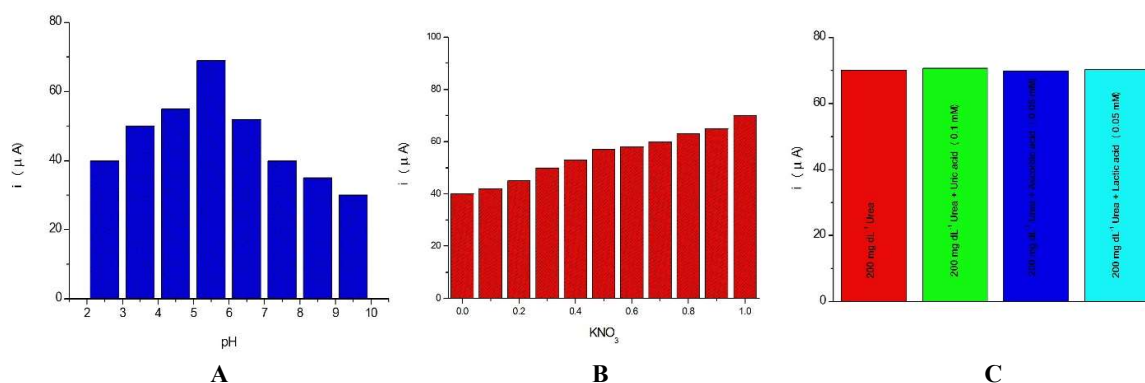

Fig. 7. (A) The influence of pH on the cyclic voltammogram electrochemical response of 200 mg dL^{-1} of urea on the Urs/CdS/SnO$_2$:F bioelectrode at E=0.2V in PBS (pH 5.5) containing 5.0 mM $[Fe(CN)_6]^{3-/4-}$ as redox probe and 1 mol L^{-1} KNO_3, and (B) The influence of KNO_3 salt concentration, as a supporting electrolyte, on the cyclic voltammogram electrochemical response of 200 mg dL^{-1} of urea on in PBS (pH 5.5) containing 5.0 mM $[Fe(CN)_6]^{3-/4-}$ as redox probe, and (C) The graph shows the effect of interferents on the CV current response of Urs/CdS/SnO$_2$:F bioelectrode

3.6. Interference study

The potential interferents influence in the urea determination was investigated under optimum situations. The potential interferents were selected from the substances which commonly present along with urea in real samples. The limit of tolerance was quantified as the

foreign substances maximum concentration, which caused an approximately ± 1 % relative error in the measurement. The result of interfering studied demonstrated that Ni^{2+}, Ca^{2+}, CN^-, Br^-, K^+, Li^+, Pb^{2+}, Mg^{2+}, Ag^+, Zn^{2+}, Mn^{2+}, Co^{3+}, Cr^{2+}, and SCN^-, glucose, sucrose, lactose, uric acid, lactic acid, ascorbic acid, and fructose have no effect on the selectivity. Fig 7C displays the effect of major interferents on the CV current response of bioelectrode. These results prove that the modified electrode has good selectivity for urea.

3.7. Analysis of real samples

Several examines were made on blood serum to survey the precision of the Urs/CdS/SnO$_2$:F bioelectrode. The urea concentration was determined by the calibration curve (Table 1). Corresponding experimentations were applied with a spectrophotometric method by a local hospital. According to the consequences, the recovery of urea is satisfactory and the consequences reproducibility is permitted by the mean relative standard deviation (R.S.D.) [7,10,29].

Table 1. Determination of urea level in blood serum

Method	Sample 1	Sample 2	Sample 3	Sample 4	Sample 5
Determined by Spectrophotometry (mg dL^{-1})	17.0 [b]	25.9	22.2	30.0 [b]	35.1
Measured by Urs/CdS/SnO$_2$:F bioelectrode (mg dL^{-1})	17.1	25.8	22.2	30.1	35.0
R.S.D. [a] (n=5) (%)	1.3	1.2	1.5	1.4	1.0

[a] R.S.D.: Relative Standard Deviation.
[b] Represents the hyper- or hypo-level of urea in blood serum, the normal urea level in blood serum is between 15 and 40 mg dL^{-1}.

3.8. The repeatability and stability of Urs/CdS/SnO$_2$:F bioelectrode

The Urs/CdS/SnO$_2$:F bioelectrode long-term stability was evaluated over a 16-weeks period. Subsequently the modified electrode was stored for 16-weeks at 4 °C temperature, the experiments were performed again. According to cyclic voltammograms, the peak potential remained unchanged and a decrement of less than 1 % compared with initial response was observed.

The modified electrode antifouling properties towards the electrochemical process and other oxidation products were deliberated by recording the CVs. Voltammograms were document in the urea attendance after cycling the potential 500 times at a scan rate of 0.1 V s^{-1} in PBS (pH 5.5) containing 5.0 mM [Fe(CN)$_6$]$^{3-/4-}$ as redox probe and 1 mol L^{-1} KNO$_3$. Consequences confirmed that peak potentials continued unchanged and the currents reduced by less than 1%. According to the results, the application of modified Urs/CdS/SnO$_2$:F provides increased sensitivity and decreased fouling effect of the analyte and electrochemical reactions product.

The proposed Urs/CdS/SnO$_2$:F bioelectrode has a less than 3 s quick response time. Our consequences of using electrochemical reactions urea bioelectrode (this work) compared with the other bioelectrodes exhibit appropriate efficiency of the fabricated bioelectrode with respect to the other bioelectrodes (Table 2). It can be assumed that the CdS nanorod demonstrates the good linear range, fast response time, and low detection limit. The fast response time can be related to the faster electron transfer at the electrode surface as described in the novel mechanism.

Table 2. Analytical characteristics of Urs/CdS/SnO$_2$:F bioelectrode compared with other reported values of urea biosensor in the literature.

Matrix	Response Characteristics			Detection method	Ref.
	DR	DL	RT		
Nano-porous silicon	10-100 mmol l^{-1}	-	<1 min	Amperometric	[39]
ZnO nanowire	0.1-100 m mol l^{-1}	0.1 m mol l^{-1}	4 s	Potentiometric	[40]
Polyaniline	10^{-6}-10^{-1} mol l^{-1}	-	-	Potentiometric	[41]
Graphite and platinum composite electrode	10-250 µ mol l^{-1}	3 µ mol l^{-1}	2 min	Amperometric	[42]
Carboxylic poly(vinylchloride)	10^{-5}-10^{-1} mol l^{-1}	0.28 m mol l^{-1}	-	Potentiometric	[43]
Polyethylenimine	10$^{-2.5}$-10$^{-1.5}$ mol l^{-1}	10$^{-2.5}$ mol l^{-1}	15-30 s	Potentiometric	[44]
Nanoporous Alumina	0.5 µM-3.0 m mol l^{-1}	0.2 µ mol l^{-1}	30 s	Conductometric	[45]
ZnO nanorods	0.001-24.0 m mol l^{-1}	10 µ mol l^{-1}	-	Cyclic Voltammetry	[46]
Carbon paste electrode modified with multi-walled carbon nanotubes (MWCNTs)	1×10^{-7}- 1×10^{-2} mol l^{-1}	52 nmol l^{-1}	-	Voltammetric	[47]
Ag on ZnO nanorod	-	13.98 µ mol l^{-1}	-	Chronoamperometric	[48]
Hypobromite solution	1-16 m mol l^{-1}	-	1 s	Chemiluminescence	[49]
Sputtered ZnO thin film	5–140 mg dl^{-1}	2.42 mg dl^{-1}	4 s	Impedimetric	[50]
Fe$_3$O$_4$-ZnO nanocomposite	5-150 mg dl^{-1}	5 mg dl^{-1}	5 s	I–V	[51]
Urs/CdS/SnO$_2$:F bioelectrode	5-200 mg dl^{-1}	3 mg dl^{-1}	3 s	Impedimetric	This work

Detection Range [DR], Detection Limit [DL], Response Time [RT]

The distinctive combination of innovative analyses with high-resolution quantitative procedures consequences with great potential for future surveys would be exploited [52-55].

4. CONCLUSION

The projected protocol revealed herein a simple, novel, inexpensive, portable and easy-to-use construction technique for the urea quantification concentrations in human blood serum and real samples with excellent analytical performance. The current examination exposed that

after modification of the SnO$_2$:F electrode with CdS nanorods, the electrochemical peak currents are meaningfully enhanced. The close enzyme-substrate contact through Urs adsorption on CdS nanorods accompany with a novel mechanism may enhance faster detection kinetics, once the electrochemically measurable species is formed nearer to the transducer, decreasing diffusion resistance, and consequently enhancing sensitivity and diminishing response times. The sensitivity and stability presented by this simple electrode pattern are high sufficient to permit the perfect measurement of low levels of urea. Comparison of the proposed bioelectrode with other electrochemical bioelectrode displays that the projected technique delivers a wider linear dynamic range. The electrode established a linear response over a broad range of urea concentrations (5 to 200 mg dL^{-1}), the detection limit was 3 mg dL^{-1} (after 3 s).

REFERENCES

[1]   M. R. Moharamzadeh, H. Salar Amoli, R. Rahmanian and S. A. Mozaffari, J. Chin. Chem. Soc. 65 (2018) 735 .

[2]   R. Rahmanian, S. A. Mozaffari, H. Salar Amoli and M. Abedi, Sens. Actuators B 256 (2018) 760.

[3]   M. Aghazadeh, A. Bahrami-Samani, D. Gharailou, M. G. Maragheh, M. R. Ganjali and P. Norouzi J. Mater. Sci. Mater. Electron. 27 (2016) 11192 .

[4]   O. Ramezani Azghandi and A. Farahbakhsh Int. J. Nano Dimens. 6 (2015) 23 .

[5]   H. Beitollahi, A. Gholami and M. R. Ganjali, Mater. Sci. Eng. C 57 (2015) 107.

[6]   J. P. Marco, K. B. Borges, C. R. T. Tarley, E. S. Ribeiro and A. C. Pereira, J. Electroanal. Chem. 704 (2013) 159.

[7]   R. Rahmanian, S. A. Mozaffari and M. Abedi, Mater. Sci. Eng. C 146 (2015) 387.

[8]   I. Karimzadeh, M. Aghazadeh, M. R. Ganjali, P. Norouzi, S. Shirvani-Arani, T. Doroudi, P. H. Kolivand, S. A. Marashi and D. Gharailou, Mater. Lett. 179 (2016) 5.

[9]   S. A. Mozaffari, H. Salar Amoli, S. Simorgh and R. Rahmanian, Electrochim. Acta 184 (2015) 475.

[10] M. Mikani, R. Rahmanian, M. Karimnia and A. Sadeghi, J. Chin. Chem. Soc. 64 (2017) 1446.

[11] S. Keyvan, E. D. Zobairi and A. Islamnezhad, Int. J. Nano Dimens. 3 (2012) 115.

[12] M. Mikani, H. Torabizadeh and R. Rahmanian, IET Nanobiotechnol. 12 (2018) 633.

[13] M. Mikani, H. Torabizadeh and R. Rahmanian, J. Chin. Chem. Soc. 65 (2018) 771 .

[14] H. Beitollahi, H. Karimi-Maleh and H. Khabazzadeh, Anal. Chem. 80 (2008) 9848.

[15] M. Mazloum-Ardakani, B. Ganjipour, H. Beitollahi, M. K. Amini, F. Mirkhalaf, H. Naeimi and M. Nejati-Barzoki, Electrochim. Acta 56 (2011) 9113.

[16] D. Odaci, A. Telefoncu and S. Timur, Sens. Actuators B 132 (2008) 159 .

[17] N.V. Suramwar, S. R. Thakare and N. T. Khaty, Int. J. Nano Dimens. 3 (2012) 75.

[18] M. Aghazadeh, R. Ahmadi, D. Gharailou, M. R. Ganjali and P. Norouzi, J. Mater. Sci. Mater. Electron. 27 (2016) 8623 .

[19] H. Gholipour-Ranjbar, M. R. Ganjali, P. Norouzi and H. R. Naderi, Ceram. Int. 42 (2016) 12097.

[20] A. Pourahmad, Int. J. Nano Dimens. 7 (2016) 121.

[21] H. Gholipour-Ranjbar, M. R. Ganjali, P. Norouzi and H. R. Naderi, J. Mater. Sci. Mater. Electron. 27 (2016) 10163 .

[22] T. Alizadeh, M. R. Ganjali, M. Zare M., and P. Norouzi, Electrochim. Acta 55 (2010) 1568.

[23] F. Chen, D. Jia, Y. Cao, X. Jin and A. Liu, Ceram. Int. 41 (2015) 14604.

[24] C. Han, M. Q. Yang, N. Zhang and Y. Xu, J. Mater. Chem. A 2 (2014) 19156.

[25] S. Mazumdar and A. J. Bhattacharyya, RSC Adv. 5 (2015) 34942 .

[26] C. C. Kocak, A. Altin, B. Aslissen and S. Koccak, Int. J. Electrochem. Sci. 11 (2016) 233.

[27] T. Alizadeh, M. R. Ganjali, M. Akhoundian and P. Norouzi, Microchim. Acta 183 (2016) 1123.

[28] G. Zhao, Y. Si, H. Wang and G. Liu, Int. J. Electrochem. Sci. 11 (2016) 54.

[29] R. Rahmanian and S. A. Mozaffari, Sens. Actuators B 207 (2015) 772.

[30] G. P. Nikoleli, M. Q. Israr, N. Tzamtzis, D. P. Nikolelis, M. Willander and N. Psaroudakis, Electroanalysis 24 (2012) 1285.

[31] S. Jakhar and C. S. Pundir, Biosens. Bioelectron. 100 (2018) 242.

[32] M. Singh, N. Verma, A. K. Garg and N. Redhu, Sens. Actuators B 134 (2008) 345.

[33] B. Kovacs, G. Nagy, R. Dombi and K. Toth, Biosens. Bioelectron. 18 (2003) 111.

[34] G. P. Nikoleli, D. P. Nikolelis and C. Methenitis, Anal. Chim. Acta 675 (2010) 58.

[35] H. C. Tsai and R. A. Doong, Biosens. Bioelectron. 20 (2005) 1796.

[36] J. Traynor, R. Mactier and C. Geddes, BMJ 333 (2006) 733.

[37] M. Žic, J. Electroanal. Chem 760 (2016) 85.

[38] C. T. Chasapis and G. Konstantinoudis, Biophys. Chem. 256 (2020) 106269 .

[39] J. H. Jin, S. H. Paek, C. W. Lee, N. K. Min and S. I. Hong, J. Korean Phys. Soc. 42 (2003) 735.

[40] S. Ali, Z. H. Ibupoto, S. Salman, O. Nur, M. Willander and B. Danielsson, Sens. Actuators B 160 (2011) 637.

[41] B. Lakard, D. Magnin, O. Deschaume, G. Vanlancker, K. Glinel, S. Demoustier-Champagne, B. Nysten, A. Jonas, P. Bertrand and S. Yunus, Biosens. Bioelectron. 26 (2011) 4139.

[42] A. Pizzariello, M. Stredansky, S. Stredanska and S. Miertus, Talanta 54 (2001) 763.

[43] Z. Wu, L. Guan, G. Shen and R. Yu, Analyst 127 (2002) 391.

[44] B. Lakard, G. Herlem, S. Lakard, A. Antoneou and B. Fahys, Biosens. Bioelectron. 19 (2004) 1641.

[45] Y. Zhengpeng, S. Shihui, D. Hongjuan and Z. Chunjing, Biosens. Bioelectron. 22 (2007) 3283.

[46] R. Ahmad, N. Tripathy and Y. Hahn, Sens. Actuators B 194 (2014) 290.

[47] T. Alizadeh, M. R. Ganjali and F. Rafiei, Anal. Chim. Acta 974 (2017) 54.

[48] J. Yoon, E. Lee, D. Lee, T. Oh, Y. Soo Yoon and D. J. Kim, J. Electrochem. Soc. 164 (2017) 558.

[49] M. Ozaki, T. Okabayashi, N. Koga, K. Sakurabu, M. Kobayashi and M. Nakagawa, Procedia Eng. 25 (2011) 960.

[50] S. A. Mozaffari, R. Rahmanian, M. Abedi and H. Salar Amoli, Electrochim. Acta 146 (2014) 538.

[51] M. Mikani, S. Talaei, R. Rahmanian, P. Ahmadi and A. Mahmoudi, J. Electroanal. Chem. 840 (2019) 285.

[52] K. Asadpour-Zeynali, S. M. Sajjadi, F. Taherzadeh and R. Rahmanian, Spectrochim. Acta A 123 (2014) 273.

[53] R. Khani, J. B. Ghasemi, F. Shemirani and R. Rahmanian, Chemom. Intell. Lab. Syst. 144 (2015) 48.

[54] S. M. Sajjadi, H. Abdollahi, R. Rahmanian and L. Bagheri, Spectrochim. Acta A 156 (2016) 63.

[55] R. Khani, R. Rahmanian and N. V. Motlagh, Food Anal. Method 9 (2016) 1112.